Impurity against non-locality in the incommensurate phase of Rb_2ZnCl_4: a ^{35}Cl NQR study

Impurity against non-locality in the incommensurate phase of Rb$_2$ZnCl$_4$: a ^{35}Cl NQR study

R K Subramanian, K Venu and V S S Sastry

School of Physics, University of Hyderabad, Central University (PO), Hyderabad 500 134, India

Abstract. The influence of impurities on the phason and amplitudon dynamics in the incommensurate phase of (Rb$_{1-x}$Cs$_x$)$_2$ZnCl$_4$ (for $x = 0.005$ and 0.01) is investigated using ^{35}Cl nuclear quadrupole resonance frequency (ν) and spin lattice relaxation time (T_1) measurements as a function of temperature. While the paraelectric-to-incommensurate transition temperature (T_I) is suppressed by about 8 K, the lock-in transition temperature (observed at 192 K in the pure compound) is not observed down to 77 K for $x = 0.01$. The observation of an additional singularity in the NQR spectrum of the $x = 0.01$ compound is explained as being due to the manifestation of non-locality of the modulation wave with respect to the region of influence of the nuclear spin probe. The phason and amplitudon contributions to the spin lattice relaxation, $T_{1\phi}$ and T_{1A} respectively, are measured by selective excitation of the broadened NQR spectra. While T_{1A} is insensitive to impurities, $T_{1\phi}$ is strongly dependent on temperature and impurity concentration. The temperature dependence of $T_{1\phi}$ is explained as being due to the underdamping of phonon modes in the presence of impurities.

1. Introduction

The theory of structurally incommensurate systems predicts the existence of a gapless acoustic-like phason branch in the incommensurate phase in addition to an optic-like amplitudon branch. In the presence of defects and impurities these systems exhibit a number of striking features, such as multi-soliton lattice, finite phason gap, pinning of the modulation wave, and so on [1, 2]. A number of compounds belonging to the A$_2$BX$_4$ family (A = K, NH$_4$, Rb; B = Zn, Cd, Hg; X = Cl, Br, I) exhibit a phase transition from a high-temperature paraelectric phase to a low-temperature incommensurate phase. Recently, there have been attempts to understand the influence of the substitution of impurities on the dynamics of the incommensurate wave, the impurities being A$_2$BX$_4$ compounds having cations of smaller size (NH$_4$ or K for Rb in Rb$_2$ZnCl$_4$) [1, 2]. Interestingly, the dopants themselves exhibit incommensurate transitions at higher temperatures with decreasing cation sizes. The addition of these non-symmetry-breaking ions has only a subtle effect on the paraelectric-to-incommensurate transition at T_I, although the low-temperature commensurate phase is destroyed for heavier doping [3].

Such studies with non-symmetry-breaking impurities having a heavier cation, for example Cs$_2$ZnCl$_4$ doped in Rb$_2$ZnCl$_4$ (having a phase transition from a paraelectric to incommensurate phase at 302 K), should prove to be very interesting and have not been attempted so far. Furthermore, Cs$_2$ZnCl$_4$ [4] does not exhibit any structural instability down to 36 K, unlike the other dopants tried earlier. Recent NQR studies of anion dynamics in the paraelectric phases of these compounds (Rb$_2$ZnCl$_4$ and Cs$_2$ZnCl$_4$) and in the doped

system $(Rb_{1-x}Cs_x)_2ZnCl_4$ ($0 \leqslant x \leqslant 0.05$) have shown that the structural stability of the paraelectric phase in this system is correlated with the dynamics of the $ZnCl_4$ anion [5, 6]. In Rb_2ZnCl_4, for example, the anions are found to experience an anharmonic double-well-type potential for their torsional motions about a Zn–Cl bond, which is nearly parallel to the *a* axis (the direction of propagation of the modulation wave in the low-temperature phase) while such anharmonicity is not evident for similar motions in Cs_2ZnCl_4. On the other hand, the converse seems to be true for such motions around axes perpendicular to this direction. Furthermore, experiments on $(Rb_{1-x}Cs_x)_2ZnCl_4$ seem to indicate that the structural stability is profoundly influenced by such perpendicular motions, whereas the parallel motions are found to be rather unimportant [6]. Unlike the smaller cations (as impurities), the presence of a Cs impurity has a dramatic effect on the anion dynamics in the paraelectric phase and on the paraelectric-to-incommensurate phase transition, suppressing the transition temperature (T_i) by almost 45 K for $x = 0.05$. Since the incommensurate phase transition is associated mainly with the rotational dynamics of these anions, it is reasonable to expect a much greater influence of such larger impurities on the dynamics of the incommensurate phase, in the above mixed system, than with smaller impurity cations. The present investigations are aimed at examining this aspect by measuring the temperature variation of the ^{35}Cl NQR frequency and spin-lattice relaxation times in the incommensurate phase of the doped system $(Rb_{1-x}Cs_x)_2ZnCl_4$ for $x = 0.005$ and 0.01.

2. Experimental details

Doubly recrystallized polycrystalline samples of $(Rb_{1-x}Cs_x)_2ZnCl_4$ ($x = 0$, 0.005 and 0.01) are obtained by slow evaporation of an aqueous solution containing the chlorides in stoichiometric ratios. The values of x quoted represent the stoichiometry of compounds used in the preparation and these samples are the same as those used for earlier studies in the paraelectric phase [6].

Measurements were carried out in the incommensurate phase on compounds with two different impurity concentrations ($x = 0.005$ and 0.01) as well as on a nominally pure compound, although similar studies on single-crystal samples of Rb_2ZnCl_4 were reported earlier [6]. Owing to the considerable broadening of the resonance lines, due to both the polycrystalline nature of the sample and the inherent inhomogeneous distribution of resonance frequencies ($T_2^* \simeq 45 \mu s$ in the paraelectric phase), a Hahn spin-echo sequence was used to observe the weak singularities expected over the broadened NQR line. The measurements were carried out on the chlorine site with the highest frequency, since its quasi-continuous spectrum spreads only by about 100 kHz, compared to about 500 kHz for the other two lines. An inversion-recovery spin-echo sequence ($\pi - \tau - \pi/2 - \tau' - \pi, \tau'$ kept constant at 180 μs) was used to measure the quadrupolar spin-lattice relaxation time corresponding to these singularities. A gas-flow-type cryostat with liquid nitrogen vapour was used for the variation of temperature, with a typical stability of 0.1 K. The temperature dependence of the position of these singularities was observed by selectively exciting different spin packets with soft pulses (typical $\pi/2$ pulse width of about 50 μs) after allowing sufficient time for temperature stabilization to minimize the temperature gradient across the sample. Spin lattice relaxation times corresponding to the different singularities were measured after an initial scan to find their location, and then by selectively exciting spins over a bandwidth of about 12 kHz around each peak, using the inversion-recovery spin-echo sequence. The accuracy in the measurement of frequency was about ± 2.5 kHz, while it was about 10% with respect to relaxation time measurements.

3. Results

The paraelectric-to-incommensurate transition temperature (T_I) observed at 302 K for the pure compound is suppressed to 298 K for $x = 0.005$ and then to 294 K for $x = 0.01$ (see table 1). The lock-in transition temperature to a low-temperature commensurate phase (T_c) is dramatically affected by the impurity, as evidenced by the shift in T_c from 192 K in the pure compound [7] to 178 K for $x = 0.005$, while no signature of such a transition (as evidenced by spectral intensity or relaxation time) is observed in the $x = 0.01$ compound, down to 77 K.

Table 1. Transition temperatures in $(Rb_{1-x}Cs_x)_2ZnCl_4$ for different values of x.

x	T_I (K)	T_c (K)
0.000	302	192
0.005	298	178
0.010	294	—

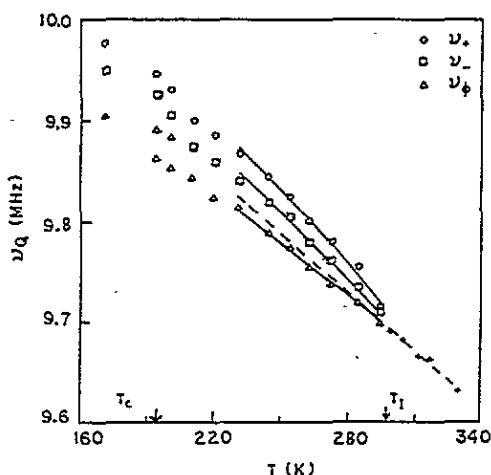**Figure 1.** Temperature variation of three singularities in the incommensurate phase of $(Rb_{1-x}Cs_x)_2ZnCl_4$ for $x = 0.00$. Full curves are the best-fit curves to equations (3a) and (3b), as explained in the text. The broken curve is the extension of the Bayer type of temperature dependence of the high-temperature paraelectric curve.

Figure 2. Temperature variation of three singularities in the incommensurate phase of $(Rb_{1-x}Cs_x)_2ZnCl_4$ for $x = 0.005$. Full curves are the best-fit curves to equations (3a) and (3b), as explained in the text. The broken curve is the extension of the Bayer type of temperature dependence of the high-temperature paraelectric curve.
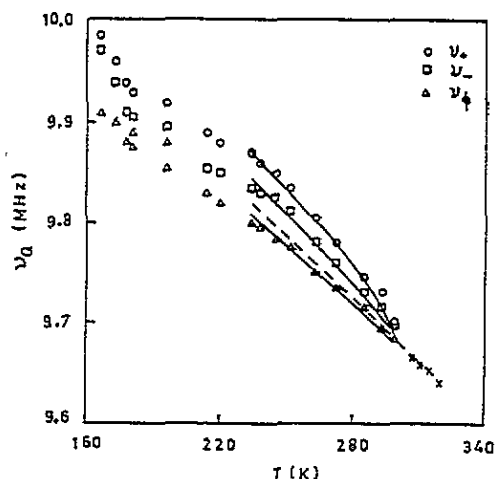
Three NQR lines are seen in the paraelectric phase corresponding to the inequivalent chlorine sites in each unit cell. When cooling from above the intensity of all the lines drops considerably. At T_I, the highest paraelectric line is broadened only by ~ 100 kHz, while the lower two lines are considerably broadened, so that they are not seen in the incommensurate phase. Hence, measurements are made only on this line. Below T_I, three singularities (ν_+, ν_- and ν_ϕ) in the otherwise inhomogeneously broadened line are observed throughout the incommensurate phase in the pure sample and compound with $x = 0.005$ (figures 1 and 2).

The lowest singularity (v_ϕ) can be linearly extrapolated to the high-temperature paraelectric phase frequency. The intensities of all three singularities decrease while cooling from T_I, and in the vicinity of T_c (about 8–10 K above) a fourth singularity is observed in both these compounds, which is found to increase in intensity with further decrease of temperature. At the transition (T_c), the singularity with the lowest frequency (v_ϕ) disappears.
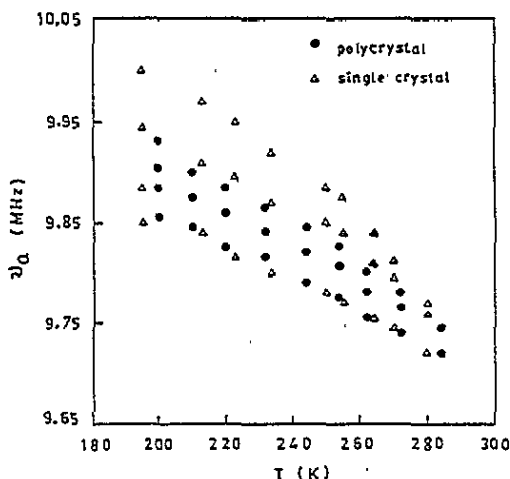

Figure 3. Comparison of the position of singularities in the NQR spectra of single-crystalline [8] and polycrystalline Rb$_2$ZnCl$_4$.
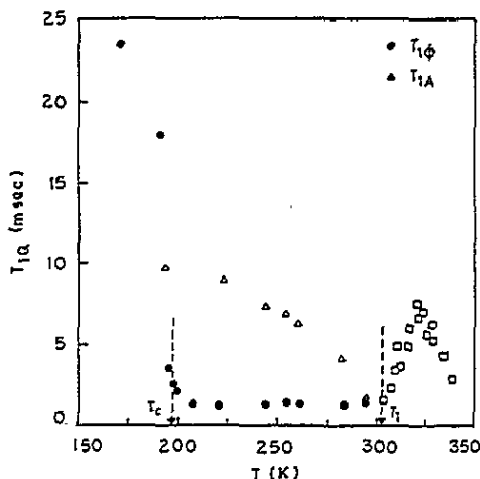
Figure 4. Temperature dependence of spin-lattice relaxation time T_{1Q} in the incommensurate phase of (Rb$_{1-x}$Cs$_x$)$_2$ZnCl$_4$ for $x = 0.00$. T_{1A} and $T_{1\phi}$ are measured at the singularities v_+ and v_ϕ respectively.

It can be seen from figure 3 that the extent of dispersion of the three singularities in the incommensurate phase is reduced by about half for the pure powder sample compared to the single-crystal data on the pure compound [8]. While the position of the lowest-frequency singularity is independent of the nature of the pure sample, the other two singularities of the polycrystalline sample (present study) are markedly below those of the single-crystal data.

Relaxation time measurements on the v_+ and v_ϕ singularities (designated as T_{1A} and $T_{1\phi}$ respectively) of the pure compound indicate that $T_{1\phi}$ is temperature independent almost throughout the incommensurate phase (with a value of about 1.2 ms), and gradually starts increasing near T_c, jumping by a factor of about five at the transition (figure 4). However, T_{1A} is dependent on temperature throughout the incommensurate phase. In the case of the doped compound ($x = 0.005$) (figure 5), $T_{1\phi}$ starts showing a temperature dependence from about 233 K and a steep variation occurs around 194 K, jumping by a factor of almost six at T_c (178 K). On the other hand, the presence of impurity does not seem to affect T_{1A}.

Four distinct singularities are observed for the $x = 0.01$ compound from almost 290 K down to 77 K (figure 6). The intensity of all four singularities drops to a minimum around 220 K, and even at 77 K no increase in intensity of any singularity is observed (figure 7). It is also found that the lowest-frequency singularity (f_1) is the weakest, while the middle two singularities (f_2 and f_3) are of almost equal intensity. The highest-frequency singularity (f_4) is slightly weaker and considerably broader than the others. The locations of the singularities corresponding to the upper three frequencies in this system ($x = 0.01$) correspond to those observed in the $x = 0$ compound (powder sample, present study), and the additional singularity appears below the lowest-frequency singularity of the pure compound (figure 8).
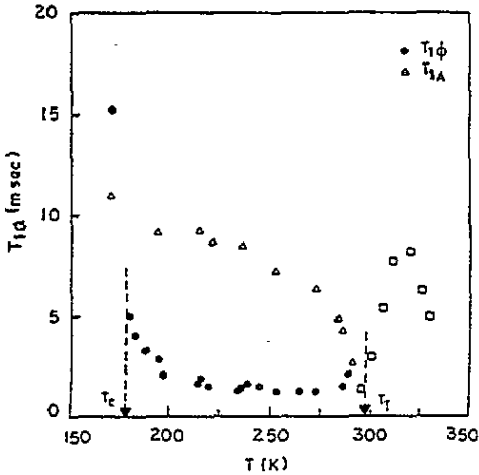
Figure 5. Temperature dependence of spin-lattice relaxation time $T_{1\varrho}$ in the incommensurate phase of $(Rb_{1-x}Cs_x)_2ZnCl_4$ for $x = 0.005$. T_{1A} and $T_{1\phi}$ are measured at the singularities ν_+ and ν_ϕ respectively.

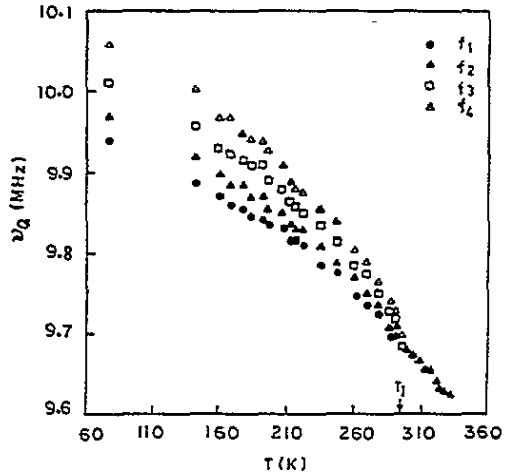**Figure 6.** Temperature variation of four singularities in the incommensurate phase of $(Rb_{1-x}Cs_x)_2ZnCl_4$ for $x = 0.01$. These four singularities, attributed to the non-local nature of the incommensurate modulation wave, are designated differently (f_1, f_2, f_3 and f_4) to distinguish them from the three singularities observed in the local case (ν_+, ν_- and ν_ϕ).

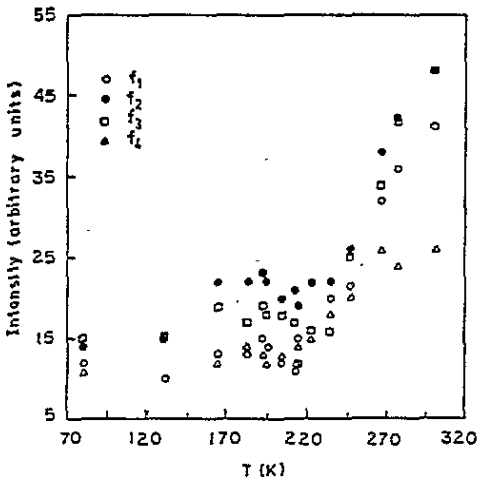**Figure 7.** Temperature variation of intensity of singularities in the incommensurate phase of $(Rb_{1-x}Cs_x)_2ZnCl_4$ for $x = 0.01$.
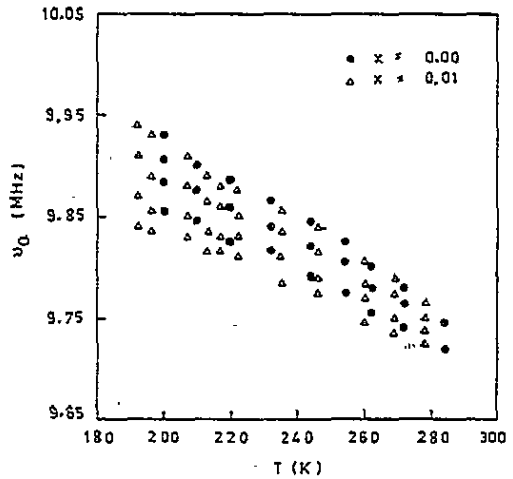
Figure 8. Comparison of position of singularities in the system $(Rb_{1-x}Cs_x)_2ZnCl_4$ for $x = 0.00$ and 0.01.

The relaxation time of the lowest-frequency singularity (f_1) (also designated as $T_{1\phi}$) for the $x = 0.01$ compound gradually increases almost from T_I (about 1.3 ms) and reaches a value of about 4.4 ms at 165 K (figure 9). $T_{1\phi}$ could not be measured at 77 K due to very weak signals. The relaxation time of the highest-frequency singularity (f_4) (designated as T_{1A}) is dependent upon temperature, and its values are almost equal to the T_{1A} of the

other two compounds ($x = 0$ and $x = 0.005$), not apparently influenced by the presence of impurities. The relaxation times of the middle two singularities (f_2 and f_3) also show a temperature dependence, although their values are smaller than that observed for f_4.

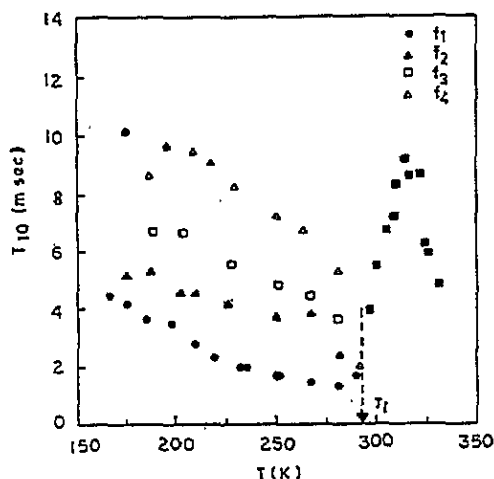**Figure 9.** Temperature dependence of spin-lattice relaxation time T_{1Q} in the incommensurate phase of $(Rb_{1-x}Cs_x)_2ZnCl_4$ for $x = 0.01$.

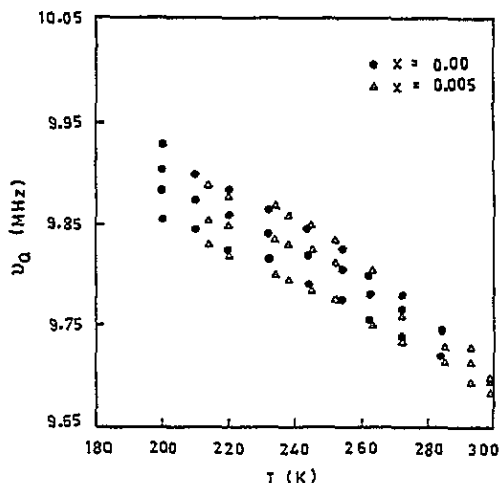**Figure 10.** Comparison of position of singularities in the system $(Rb_{1-x}Cs_x)_2ZnCl_4$ for $x = 0.00$ and 0.005.

4. Discussion

4.1. $(Rb_{1-x}Cs_x)_2 ZnCl_4$ for $x = 0$ and 0.005

4.1.1. Temperature dependence of NQR frequencies. The observation of three singularities for $x = 0$ and 0.005, wherein the position of the lowest-frequency singularity is essentially independent of temperature (but for the usual Bayer-type of temperature dependence) while the other two are critically dependent on temperature, is a manifestation of the onset of the incommensurate phase and can be explained by expanding the resonance frequency in powers of the order parameter in the local approximation [9]. The relevant order parameter in this system characterizing the displacement of the nuclei is expressed as $u = A \cos \phi(x)$ in the plane-wave limit. Here A is the amplitude of the incommensurate modulation wave and ϕ is the phase. In this limit the resonance frequency is written as

$$\nu = \nu_0 + \nu_1 \cos \phi + \tfrac{1}{2}\nu_2 \cos^2 \phi + \dots \tag{1}$$

where $\nu_1 \propto A$ and $\nu_2 \propto A^2$, and A shows a critical temperature dependence $(T_I - T)^\beta$. The frequency distribution function of the NQR signal

$$f(\nu) = \frac{\text{constant}}{(d\nu/d\phi)} \tag{2}$$

will have peaks whenever $d\nu/d\phi$ becomes zero. In the constant-amplitude approximation three singularities will thus appear, at

$$\nu_\pm = \nu_0 \pm \nu_1 + \tfrac{1}{2}\nu_2 \tag{3a}$$

Table 3. Comparison of computed parameters at 255 K in different systems.

	$x = 0.00$ (Polycrystalline)	$x = 0.00$ (Single crystal)	$x = 0.005$ (Polycrystalline)
ν_1	1.0×10^{-2}	2.8×10^{-2}	1.3×10^{-2}
ν_2	3.9×10^{-2}	7.4×10^{-2}	4.7×10^{-2}
ν_1/ν_2	0.25	0.37	0.26

corresponding to $\cos\phi = \pm 1$, and

$$\nu_\phi = \nu_0 - \nu_1{}^2/4\nu_2 \tag{3b}$$

corresponding to $\cos\phi = 0$. The ν_ϕ singularity is due to the non-linearity in the relation between the NQR frequency and the order parameter.

The edge singularities $\nu_\pm$ (corresponding to $\cos\phi = \pm 1$) depend critically on the order parameter due to the presence of ν_1 and ν_2, and their positions change significantly while cooling into the incommensurate phase. An estimate of the critical exponent β characterizing the phase transition can be made by observing the temperature dependence of the splitting between the two edge singularities, since

$$\Delta\nu = \nu_+ - \nu_- = 2\nu_1 \propto (T_I - T)^\beta. \tag{4}$$

On the other hand, the frequency and width of the line ν_ϕ (corresponding to $\cos\phi \simeq 0$) are expected to be nearly independent of temperature. However this singularity, like others, will continue to exhibit a Bayer-type temperature dependence.

Although this description is valid almost throughout the incommensurate phase, due to the formation of commensurate regions ($d\phi/dx = 0$) near the lock-in transition, one may expect to find additional singularities (breakdown of the plane-wave limit [9]). These are expected to increase in intensity at the expense of those due to incommensurate modulation, and at the lock-in transition the intensity of the latter singularities tends to zero. The number of lines observed in the low-temperature lock-in phase will reflect the change in symmetry compared to the high-temperature paraelectric phase.

The three observed singularities (figures 1 and 2) fit this description throughout the incommensurate phase. The analysis of the data is carried out by first computing ν_1 at each temperature in the incommensurate phase using (4), and then ν_2 (equations (3a) and (3b)) with the criterion $\nu_1 < \nu_2$; ν_0 is then trivially determined. These values at different temperatures are used to determine A_0, B_0 and β according to

$$\nu_1 = A_0(T_I - T)^\beta \tag{5a}$$
$$\nu_2 = B_0(T_I - T)^{2\beta} \tag{5b}$$

and the results are summarized in table 2. It is seen that the presence of an impurity ($x = 0.005$) does not seem to affect the amplitude of the modulation wave to any appreciable extent, as evidenced by the comparable values of A_0 and B_0 in both cases (table 2). This is also clear from figure 10.

Table 2. Best-fit parameters obtained using (5).

	$x = 0.000$	$x = 0.005$
β	0.34	0.35
A_0	2.8×10^{-3}	3.2×10^{-3}
B_0	2.6×10^{-3}	4.6×10^{-3}

Table 3 shows the values of ν_1, ν_2 and ν_1/ν_2 at an arbitrary temperature (255 K) in both the single-crystal and polycrystal samples of the pure compound and those for $x = 0.005$. The considerable reduction in all the parameters from single crystal to powder suggests that the amplitude of displacement is reduced in the powdered sample (figure 3). Since single-crystal data were satisfactorily analysed in [8] using an expansion of the frequency up to the second-order term in the order parameter, the present analysis seems justified and adequate. The full curves in figures 1 and 2 show the fitting of the data to the above model down to the temperature where the plane-wave model is valid. The broken curve indicates the variation of ν_0 with temperature, as obtained from the above analysis (the best fit to the Bayer type of temperature dependence).

The observation of an additional singularity near T_c indicates the formation of a multi-soliton lattice. The increase in intensity of this singularity (corresponding to a commensurate region, $d\phi/dx = 0$) shows that the soliton density is decreasing and the commensurate regions are increasing at the expense of soliton regions with a decrease in temperature. While the $\nu_\pm$ singularities are observed even below T_c, ν_ϕ disappears at the transition. The observation of three lines in the commensurate phase indicates the triplication of the high-temperature unit cell edge. Apart from indicating that the lock-in transition temperature for the $x = 0$ compound is not affected by the nature of the sample, the data also show that T_c is shifted from 192 K to 178 K with a 0.5% substitution of impurities.

4.2. Temperature dependence of relaxation times

In contrast to translationally periodic systems, the relaxation rate varies over the entire inhomogeneously broad NQR line in the incommensurate phase due to the contribution to relaxation from the two excitation spectra of the incommensurate modulation wave, namely the amplitudon and phason at different parts of the NQR spectrum. An analysis based on a detailed theoretical model allows for the estimation of these two contributions. By considering relaxation via direct one-phason and one-amplitudon processes, the spin transition probability can be obtained as [9]

$$W = \text{constant} \times [\cos^2 \phi(x) J_A(\omega) + \sin^2 \phi(x) J_\phi(\omega)] \tag{6}$$

where $J_A(\omega)$ and $J_\phi(\omega)$ represent spectral density functions corresponding to the amplitudon and phason fluctuations respectively. The amplitudons dominate the relaxation at nuclear sites with $\cos^2 \phi(x) = 1$ and hence at ν_+. Thus T_{1A} measured at ν_+ essentially corresponds to the amplitudon contribution. Since the amplitudons are optic like, the edge singularities exhibit a critical temperature dependence, as evidenced by the variation of relaxation rates over the incommensurate phase. On the other hand, phasons mediate the relaxation for nuclear sites with $\cos^2 \phi(x) = 0$ and hence in the centre of the distribution. Thus $T_{1\phi}$ measured at ν_ϕ is the relaxation time associated with phasons. Since the phasons are acoustic like, $T_{1\phi}$ is expected to be low and independent of temperature in nominally pure systems.

Figure 4 shows the NQR spin-lattice relaxation times ($T_{1\varrho}$) at the two singularities ν_+ and ν_ϕ observed in polycrystalline Rb$_2$ZnCl$_4$. Although the T_{1A} of the present system is smaller (about 8 ms at 260 K) compared to that of single crystals (about 15 ms at 260 K), the variation of its relaxation over the incommensurate phase is essentially similar (this value is also quoted at 9 ms in the literature [10]). In the vicinity of T_c the plane-wave model breaks down due to the formation of commensurate regions (multi-soliton lattice) leading to the splitting of the phason excitation spectrum into two modes, namely optic-like modes arising from the commensurate regions and acoustic-like modes resulting from incommensurate

regions. At T_c, the acoustic-like branch disappears (as the density of solitons tends to zero) and hence $T_{1\phi}$ is expected to show a sudden increase at the transition temperature [9]. The observed increase in $T_{1\phi}$ and its temperature dependence is associated with the splitting of the phason spectrum.   As the commensurate regions become large (increase in intersoliton distance), the contribution to $T_{1\phi}$ from optic-like phasons increases, and at the transition the contribution from acoustic-like phasons becomes zero (as seen by the sudden jump in $T_{1\phi}$).

The $x = 0.005$ compound also shows three singularities (figure 2).   The $T_{1\phi}$ and T_{1A} can be found by selectively exciting the ν_ϕ and ν_+ singularity in this case as well. The appearance of an additional singularity around 265 K, the disappearance of the lowest singularity around 177 K and the rapid changes in slopes of the resonance frequency with temperature all indicate that the lock-in transition temperature is suppressed to about 178 K in the $x = 0.005$ compound from the 192 K observed in the pure compound. As can be seen from figures 4 and 5, the transition from the incommensurate to lock-in commensurate phase is not as sharp as observed in the pure compound. This can be understood by reasoning that, in the presence of impurities, acoustic-like phasons are not completely destroyed even at the transition, as was the case with the pure compound. The data indicate clearly the sensitivity of T_c to impurity concentration, and is in sharp contrast to such effects with smaller impurity cations [1]. T_{1A} is unaffected by the presence of impurities, while $T_{1\phi}$ sharply increases from about 4 ms at 183 K to about 15 ms at 171 K.

4.3. $(Rb_{1-x}Cs_x)_2 ZnCl_4$ for $x = 0.01$

4.3.1. Temperature dependence of the NQR frequency. Figure 6 indicates that four distinct singularities are observed down to 77 K in this compound, unlike in the earlier systems. The additional singularity observed can in principle be accounted for either by including higher-order terms of the order parameter (1) or by invoking the non-local approximation [11]. It was mentioned in the earlier discussion that the amplitude of the modulation is relatively insensitive to impurity concentration at $x = 0.005$. It is then perhaps reasonable to expect no dramatic changes in this amplitude even at $x = 0.01$. It thus seems physically unrealistic to try accounting for the additional singularity (with $x = 0.01$) by including higher-order terms. Moreover, the presence of an impurity (especially a heavier one) is expected to pin down the modulation wave very effectively and hence lead to a relatively more rapid variation in the phase of the modulation wave between impurity . Thus the non-local nature of the modulation wave seems to be an appropriate description for the lineshape analysis and relaxation time data.

In the non-local approximation, the resonance frequency at a given site is not only due to the displacement of the nucleus under consideration, but is also due to relative displacements of nearby nuclei at other positions. The resonance frequency in such a case can be written as [11]

$$\nu(x) = \nu_0 + \nu_1 \cos[\phi(x) + \phi_1] + \nu_2' + \nu_2 \cos^2[\phi(x)] + \ldots \tag{7}$$

where ν_0 corresponds to the extrapolated value (Bayer model) of the high-temperature phase NQR frequency, $\nu_1 \propto (T_I - T)^\beta$ while ν_2 and ν_2' vary as $(T_I - T)^{2\beta}$ and ϕ_1 is the phase difference between the linear and quadratic terms. The shape of the spectrum and the number of edge singularities will strongly depend on the ratio between the magnitudes of the linear and quadratic terms and the relative phase shift between these two terms. However, for

$$\tfrac{1}{2} \leqslant \nu_2/\nu_1 \leqslant 1 \qquad \phi_1 \neq 0, 90° \tag{8}$$

four singularities are to be observed. The position of the additional singularity and the values of v_2/v_1 at which they appear depend on ϕ_1. For example, if $\phi_1 = 45°$ the additional singularity appears at the centre of the two edge singularities [11].

The present results indicate four singularities down to 77 K with no discernible change in slope of the frequency against temperature plot, nor any marked variation in intensities. From figure 8 it is seen that the position of the upper three singularities are in the same location as observed in the pure compound, while the additional singularity (f_1) appears below the lowest-frequency singularity of the pure compound. This suggests that the contribution from the linear term on the modulation wave perhaps becomes considerable with increasing impurity concentration. The singularity f_1 is essentially an extension of the paraelectric line, although minor deviation from such extrapolations are observed at lower temperatures. The interesting observation is that the singularities corresponding to the edges (amplitudons) seem to have split further. Lineshape analysis carried out by considering the variation of the mean square amplitude of fluctuations of the modulation wave (which can be correlated with the distance between pinning centres) has indicated that line-broadening effects with characteristic singularities can be expected in the non-local case [12]. Interestingly, down to the lowest investigated temperature (77 K) no marked variations in the intensity of any of the singularities or any slope changes have been observed, indicating that there is no evidence for a further transition to a commensurate phase in the near vicinity. The absence of a lock-in phase transition could be due to the pinning force exerted on the incommensurate regions by the impurity atoms. This force, which is random in nature, acts to disturb the regular array of discommensurate regions near T_c, where the soliton lattice becomes soft due to the weakening of soliton–soliton interactions. Such stabilization of the incommensurate phase has also been observed in the $(Rb_{1-x}K_x)_2ZnCl_4$ system for $0.1 \leqslant x \leqslant 0.9$ [13].

4.3.2. Temperature dependence of relaxation times. The spin relaxation process mediated by amplitudon and phason branches in the non-local case is complicated due to the fact that for each value of frequency there are two distinct spin transition probabilities, resulting in the observation of non-exponential recovery of magnetization [11]. The spin-lattice relaxation times measured for all the four singularities down to 165 K are shown in figure 9. It is seen that while the relaxation time is least for the f_1 singularity (which seems to be an extrapolation of the high-temperature line), it is maximum for f_4 at any given temperature in the incommensurate phase. The higher three singularities f_2, f_3 and f_4 show a critical temperature dependence almost throughout the incommensurate phase, indicating that the optic-like amplitudons are mediating their relaxation and hence the T_1 measured for f_4 can be attributed mainly to amplitude fluctuations (T_{1A}). On the other hand, $T_{1\phi}$ measured at f_1, which can be attributed to phason contributions, as argued in the earlier case, shows a temperature dependence almost from the paraelectric to incommensurate transition temperature (1.3 ms) down to 165 K (4.4 ms). The observed temperature dependence for the phason-relaxed singularity can be thought of as being due to the formation of optic-like phasons (commensurate regions) almost right from T_1. The gradual increase in the phason relaxation time with decreasing temperature indicates that the commensurate regions are increasing, and hence the inter-soliton distance. Since the phasons are pinned at impurity centres, the continuum approximation is no longer valid as the lattice becomes discrete. This leads to the underdamping of phason branches in the spectrum, resulting in the inefficiency of direct one-phonon processes mediating the relaxation (which is expected to be temperature independent). Thus with increased pinning, anharmonic Raman processes, which are strongly dependent on temperature, mediate the relaxation for the phason-relaxed

singularity [9, 14]. It is clear that the spin transition probabilities for the direct processes, which are proportional to the number of phasons available at the resonance frequency (low compared to lattice frequencies), decrease due to the pinning of the modulation wave. On the other hand, the amplitudon branch exhibits a similar behaviour to that observed in the other compounds, indicating perhaps the insensitivity of the amplitudon branch to impurities. The expected non-exponentiality of the relaxation rates (in the non-local case) could not be observed over the distribution, possibly for several reasons, such as cross relaxation among several parts of the spectra and finite resolution of the spectrometer in exciting a single spin packet. It could also be that the dynamic environment of several spin packets, which have the same resonance frequency (static effect) and which differ in principle in their relaxation paths due to non-locality, might not be adequately different, due to cross-relaxation effects, so as to produce observable distinct relaxation processes with distinctly resolvable relaxation times. Finally, the fact that the f_1 singularity does not show any critical temperature dependence (either in position or relaxation times) perhaps suggests that this additional singularity could be due to the phason spectrum.

The observation of $T_{1\phi}$ to be only about 4.4 ms even at 165 K indicates that the acoustic-like phason (and hence broad solitons) are still dominant in mediating the relaxation processes. Thus the addition of a Cs impurity seems to have a profound effect on the dynamics of the incommensurate modulation wave, in contrast to the rather negligible influence of lighter impurities.

5. Phason gap

In a nominally pure crystal, the incommensurate phase is a floating phase and no energy is needed to excite a phason [9]. However, due to the inherent discreteness of the lattice and due to defects and imperfections, there will always be a finite gap in the phason spectrum. While the amplitudon gap is expected to be temperature dependent due to its optic-like nature, the phason gap is temperature independent because it is acoustic like. Spin-lattice relaxation measurements directly give the estimates of these gaps. In the plane-wave limit, when the relaxation is mediated by one-phason and one-amplitudon processes, the relaxation rates (phason gap $\Delta_\phi \gg \omega_Q$) can be written in terms of the respective gaps as [11]

$$T_{1\phi}^{-1} = C\frac{\pi}{4}k^{-3/2}\frac{\Gamma_\phi}{\Delta_\phi} \tag{9}$$

$$T_{1A}^{-1} = C\frac{\pi}{4}k^{-3/2}\frac{\Gamma_A}{\Delta_A} \tag{10}$$

where C is a constant proportional to the square of the fluctuating electric field gradient tensor, and Γ_ϕ and Γ_A are the phason and amplitudon damping constants respectively.

In the mean-field approximation, Δ_A represents the temperature-dependent energy gap in the amplitudon spectrum and is given by

$$\Delta_A = K_2\sqrt{(T_I - T)} \tag{11}$$

where K_2 is a constant. Since Δ_A is of the order of phonon frequency at temperatures different from T_I, and since $\Gamma_\phi = \Gamma_A = \Gamma$ and $\omega_Q \ll \Gamma \ll \Delta_A$, the individual relaxation times due to the amplitudon and phason fluctuations can be written as

$$\frac{T_{1\phi}}{T_{1A}} = \frac{\Delta_\phi}{\Delta_A}. \tag{12}$$

Thus, it is seen that from a known amplitudon gap, Δ_A, at a given temperature [15] an estimate of the phason gap can be made from the ratios of the corresponding relaxation times. The temperature dependence of the amplitudon gap can be obtained by fitting the corresponding relaxation time data to the following equation:

$$T_{1A} = K_1 \Delta_A = K_1 K_2 \sqrt{T_I - T}. \tag{13}$$

From neutron scattering measurements in Rb_2ZnCl_4, the amplitudon gap was estimated to be 0.256×10^{12} s^{-1} [15], which corresponds to a T_{1A} value of 15 ms [8]. Using these values, K_1 is found to be 58.594×10^{-12}. The temperature dependence of the amplitudon gap is calculated using (13), and the temperature dependence of the phason gap is then obtained using (12).
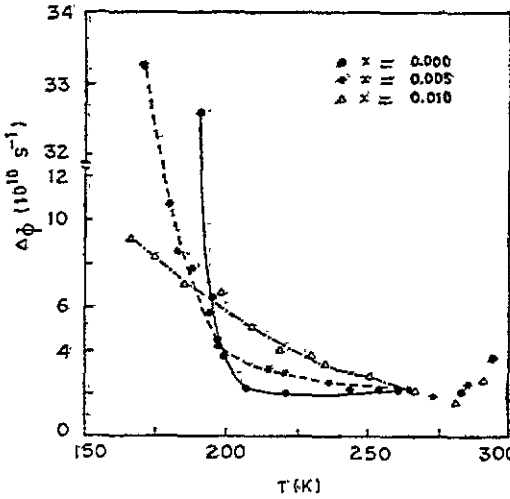

Figure 11. Temperature dependence of the phason gap Δ_ϕ in $(Rb_{1-x}Cs_x)_2ZnCl_4$ for $x = 0.00$, 0.005 and 0.01 calculated using (12) as explained in the text. The curves drawn through these points are guides to the eye.

The temperature variation of the phason gap in all three compounds is shown in figure 11. For the pure compound, the phason gap remains temperature independent almost throughout the incommensurate phase (2.1×10^{10} s^{-1}) and starts to increase about 8 K below the lock-in transition temperature. At T_c, the phason gap jumps to 6.5×10^{10} s^{-1} and is 32×10^{10} s^{-1} at 191 K, clearly indicating the disappearance of the acoustic-like phasons. On the other hand, in the $x = 0.005$ compound, Δ_ϕ starts increasing slowly from 220 K and there is a discontinuous jump by almost four times between 180 K and 171 K, indicating the decrease in the lock-in temperature. In the $x = 0.01$ compound, the phason gap increases from T_I and even at 166 K its value is only 9.2×10^{10} s^{-1}, indicating the absence of a lock-in transition until this temperature. The temperature dependence of the phason gap can be understood as being due to the underdamping of the phason excitation spectrum (resulting from pinning effects due to impurities). The temperature dependence for the phason gap even at higher temperatures with increasing impurity concentration may perhaps be due to the formation of optic-like phasons very early. The phason gap data clearly show that the transition from the incommensurate to the low-temperature commensurate phase is smeared out in the presence of impurities. The computed temperature and impurity concentration dependencies of the phason gap could be fitted to the equation

$$\Delta\phi \propto (T_I - T)^{\beta(n-2)} n_i^{0.5} \tag{14}$$

where n_i is the impurity concentration. This fit results in $\beta(n-2)$ being close to $\frac{4}{3}$ in Rb_2ZnCl_4 [16, 17].

6. Conclusions

(i) The presence of a Cs impurity in Rb_2ZnCl_4 results in the suppression of the lock-in transition by almost 15 K with a moderate concentration of $x = 0.005$, while with $x = 0.01$ such a transition is not observed down to 77 K. It is also observed that the lock-in transition is smeared in the presence of this impurity. These results suggest a strong influence of the heavier cation impurity on the stability of the paraelectric phase in comparison with similar observations with smaller-cation impurities.

(ii) The amplitudon excitations in the incommensurate phase seem to be insensitive to impurities.

(iii) The observation of four singularities from T_I down to 77 K in the $x = 0.01$ system seems to indicate a rapid phase variation of the modulation wave between impurity pinning centres in the presence of impurities, leading to observable non-local effects on the pure NQR spectrum.

(iv) The amplitude of the modulation wave in the incommensurate phase seems to be reduced, due to the polycrystalline nature of the sample in comparison to single crystals. Interestingly, while the position of the phason-relaxed singularity is insensitive to the nature of the sample, the positions of the amplitudon-relaxed singularities are sensitive to the nature of the sample.

(v) The dependence of the phason relaxation time on both impurity concentration and temperature indicates that the direct process (in the continuum lattice) becomes inefficient in the presence of impurities. In such a case, due to the presence of underdamped phasons, indirect Raman processes (dependent on temperature and impurity concentration) appear to become the dominant relaxation mechanism, leading to an increase in the phason gap.

References

[1] Milia F, Papavassiliou G and Giannakopoulos E 1990 *Z. Naturf.* **45** 323
[2] Milia F, Papavassiliou G and Giannakopoulos E 1989 *Phys. Rev.* B **39** 12 349
[3] Milia F and Papavassiliou G 1990 *Geometry and Thermodynamics* ed J C Toledano (New York: Plenum) p 429
[4] Wong P T T 1976 *J. Chem. Phys* **64** 2186
[5] Subramanian R K, Venu K and Sastry V S S 1994 *J. Phys.: Condens. Matter* **6** 137
[6] Subramanian R K, Venu K and Sastry V S S 1994 *J. Phys.: Condens. Matter* **6** 2377
[7] Gupta S K, Gladkii V V and Krishan L 1992 *J. Phys.: Condens. Matter* **4** 855
[8] Milia F and Papavassiliou G 1989 *Phys. Rev.* B **39** 4467
[9] Blinc R 1981 *Phys. Rep.* **79** 331
[10] Chen S and Ailion D C 1989 *Solid State Commun.* **69** 1041
[11] Blinc R, Prelovsek P, Rutar V, Seliger J and Zumer S 1986 *Incommensurate Phases in Dielectrics* vol 1, ed R Blinc and A P Levanyuk (Amsterdam: North-Holland)
[12] Kogaj M, Zumer S and Blinc R 1984 *J. Phys. C: Solid State Phys.* **17** 2415
[13] Hamano K 1986 *Incommensurate Phases in Dielectrics* vol 1, ed R Blinc and A P Levanyuk (Amsterdam: North-Holland)
[14] Chen S and Ailion D C 1989 *Phys. Rev.* B **40** 2332
[15] Zeyen C M E 1983 *Physica* B **120** 283
[16] Blinc R, Dolinsek J, Prelovsek P and Hamano K 1986 *Phys. Rev. Lett.* **56** 2387
[17] Prelovsek P 1988 *Phase Transitions* **11** 203